MYTRIBOS Malaysian Tribology Society
Jurnal Tribologi
Website : jurnaltribologi.mytribos.org e-issn: 2289-7232

Performance analysis of a new design concept of journal bearing with surface roughness

Mohammad Tauviqirrahman *, J. Jamari, Budi Setiyana, M. Muchammad, Danang Prabowo

Mechanical Engineering Department, Diponegoro University, Semarang 50275, Central Java, INDONESIA.
* Corresponding author: mtauviq99@yahoo.com

KEYWORDS

Acoustic
CFD
Journal bearing
Lubrication
Surface roughness

ABSTRACT

The current mechanical industries rely heavily on automatic machinery, which is generally of the rotating variety. These machines must frequently run at high speeds and under large loads for extended periods. To do this, engineers must create machines with increased load-bearing capacity, decreased friction, and lower noise levels. This study aims to investigate the performance of modified bearing including the generated noise. This bearing represents a new concept of contacting surface by introducing the roughness which is partially applied on the stationary surface of the bearing. An objective of this study is to study a possible alternative to conventional bearing, with the aim of reducing the bearing noise and improving the load support without compromising friction. The performance assessment is conducted using computational fluid dynamics (CFD) varying the surface roughness level. The computational simulations confirm that the proposed modified bearing can reduce the bearing noise, enhance the load support and decrease the friction significantly.

1.0 INTRODUCTION

The applied force is fully sustained by the pressure of the lubricating layer in a journal bearing, one of the most crucial friction pairs in machine parts. The primary function of the bearing is to maintain constant rotation of the shaft about its axis by minimizing friction between the two surfaces and damping vibrations caused by the rotation of the shaft and motor (Malcolm &

Received 19 July 2022; received in revised form 21 Novemver 2022; accepted 12 February 2023.
To cite this article: Tauviqirrahman et al. (2023). Performance analysis of a new design concept of journal bearing with surface roughness. Jurnal Tribologi 38, pp.1-18.

Leader, 2001). In recent decades, a substantial amount of research on surface modification through texturing has been conducted and continues to be conducted. This is mostly due to the fact that surface texturing has become a viable method for enhancing journal bearing performance (Gropper et al., 2016).

In addition, there are much more studies on bearing performance in relation to surface roughness. Javorova (2010) proved the usefulness of surface roughness inclusion for bearing performance analysis using the Reynolds equation. Using Cristensen's stochastic roughness theory, Hsu et al. (2013) investigated the influence of two types of surface roughness directions, longitudinal and transverse, under a magnetic field on the operational performance of bearings. They demonstrated that by increasing longitudinal roughness, load-carrying capacity can be increased. On the other hand, when transverse roughness was utilized, the opposite impact was observed. For the bearing with a slip/no-slip pattern, Kalavathi et al. (2016) constructed the generalized Reynolds equation by including Christensen's stochastic theory and addressing the roughness nature. They determined that roughness has a significant effect on the load-carrying capability. It was confirmed that surface roughness increases load-carrying ability. Cui et al. (2018) later investigated the influence of surface roughness on the transient behavior of hydrodynamic journal bearings during starting. They discovered that the longitudinal surface arrangement has a considerable impact on the hydrodynamic force reduction. Al-Samieh (2019) investigated the influence of surface roughness in sinusoidal waviness terms for Newtonian and non-Newtonian lubricants. It has been discovered that when the amplitude of the waviness grows, the pressure distribution fluctuates more. Later, Tauviqirrahman et al. (2021) revealed that engineered surface roughness in the heterogeneous rough/smooth pattern increases hydrodynamic pressure and thus load-carrying capacity. However, it was also found that the characteristic of the resulted friction is not as good as load carrying capacity. Recent research by Gu et al. (2021) suggests that surface roughness should be considered while optimizing surface texture. In addition to the surface texture, the surface roughness has a major impact on the tribological performance of the journal bearing.

Using the computational fluid dynamics (CFD) method, this paper investigates the enhancement of journal bearing performance by introducing the surface roughness, with an emphasis on improving tribological indices and strengthening the acoustical performance (i.e. low noise). The lubrication performance can be enhanced by constructing an engineered heterogeneous bearing surface on which the roughness is placed in certain areas but smooth in others. In order to capture cavitation phenomena occurring in the bearing in a more accurate manner, the multi-phase cavitation technique (Morris et al., 2019; Sun et al., 2019) is utilized in this investigation. Moreover, based on a scan of the relevant literature, significant advances in the study of roughened journal bearings have mostly focused on tribological features. Few researchers have investigated the relationship between surface roughness and bearing noise. In addition to the tribological performance, the acoustic feature of bearings is of special importance in this study.

2.0 METHOD

In this study, the flow behavior produced by surface motion is addressed using the Navier–Stokes theory for incompressible flow instead of the Reynolds theory. In this investigation, the Reynolds-averaged Navier–Stokes (RANS) equation is combined with the equation for mass

conservation. Assuming isothermal lubrication conditions simplifies the computational processing.

The RANS (momentum) equation is as follows:

$$\frac{\partial}{\partial x_i}\left(\rho u_i u_j\right) = -\frac{\partial p}{\partial x_i} + \frac{\partial}{\partial x_j}\left[\mu\frac{\partial u_i}{\partial x_j} - \rho\overline{u_i' u_j'}\right] \tag{1}$$

The mass conservation equation is:

$$\frac{\partial}{\partial x_i}(\rho u_i) = 0 \tag{2}$$

where ρ is the density of the lubricant; u_i and u_j are the average velocity components for the coordinate *x*, *y*, and *z; p* is the hydrodynamic pressure; μ is the viscosity; u_i' and u_j' are the fluctuation velocities; and $-\rho\overline{u_i' u_j'}$ is the Reynolds stress. In the current investigation, the standard model of turbulent kinetic energy *k* and turbulent dissipation rate ε_d is used to solve the Reynolds stress. Once the hydrodynamic pressure is calculated using Equations (1) and (2), in terms of tribological performance, the load-carrying capacity of the bearing can be calculated by integrating the hydrodynamic pressure acting on the bearing surface, while the friction force exerted by the lubricant on the surface can be calculated by integrating the shear stress over the surface area. In the analysis of acoustic, bearing noise is of particular interest. Due to lubrication turbulence, bearing action tends to be accompanied by noise. In this study, a computational method for resolving the noise generated by the lubricant makes use of the broadband noise source model (ANSYS, 2019). The acoustic power level P_A is denoted as follows:

$$P_A = a_e \rho \varepsilon_d \left(\frac{\sqrt{2k}}{a_0}\right)^5 \tag{3}$$

In this particular investigation, the mixture model of cavitation that is provided by CFD software is used. The mixture model depicts a vapor–liquid two-phase flow by presuming that the liquid phase changes into the vapor phase when the lubricant film pressure drops below the saturation pressure. This allows the model to illustrate the flow of vapor–liquid mixtures. Calculations are also done utilizing this method to determine the growth of gas bubbles, which is a common occurrence during the cavitation process. To integrate the cavitation effect, the Zwart–Gelber–Belamri model is utilized, in which the formation of cavities is restricted to a finite-size junction.

The sand-grain model is used to define the roughness profile of the rough surface of the heterogeneous rough/smooth bearing in the present investigation. Here, a monolayer of spheres is utilized to cover the surface evenly. Utilizing the modified law-of-the-wall for mean velocity, surface roughness is modeled. This equation may also be written as (ANSYS, 2019):

$$\frac{u_p u^*}{\tau_w / \rho} = \frac{1}{\kappa} \ln\left(E \frac{\rho u^* y_p}{\mu} \right) - \Delta B \tag{4}$$

where $u^* = C_\eta^{1/4} k^{1/2}$ and $\Delta B = (1/\kappa) \ln f_r$. For sand-grain roughness, ΔB is affected by the physical roughness height K_s, while the height is assumed constant per surface (ANSYS, 2019). According to Adams et al. (2012), to correlate the roughness height K_s with the average roughness R_a, the following equation can be applied:

$$K_s = 0.5863 R_a \tag{5}$$

This equation permits the effect of the surface's geometrical average roughness R_a to be computed. In real, the R_a is frequently measured by a profilometer. In this investigation, homogeneous sand grain roughness is assumed for simplicity.

3.0 CFD MODEL

In this work, the notion of the heterogeneous rough/smooth bearing is introduced, in which the rough condition is applied to only a portion of the bearing's surface. Numerically, the heterogeneous roughness distribution is modeled by applying the surface boundary condition to the selected area and inputting the sand-grain roughness value K_s to represent the roughness. As input to the CFD program, the surface profile will be used to determine the lubricant film thickness. Figure 1 represents the schematic of the new design of water-lubricated journal bearing with the partially roughened zone. Table 1 shows the journal bearing geometry as well as the lubricating water properties.

For new designs of journal bearings, the roughness is applied to a specific section of the bearing, ranging from 0 to 180 degrees. Similar to the concept of surface texturing, the current approach is inspired by the observation that altering the fluid film properties of lubricated journal bearings by artificial surface roughness improves bearing performance. The parameter R_a (the average roughness) is used to represent the surface roughness level. As seen in Table 1, R_a is of particular interest for various roughness values.

In this work, the numerical mesh of the journal bearing is built via ANSYS meshing function. As illustrated in Table 2, face-meshing, edge-sizing, and sweep methods are used to construct a mesh configuration. the generated mesh on journal bearings is developed as depicted in Figure 2. The developed mesh is comprised of a homogeneous hexahedral grid. The number of fluid layers in the radial direction is the refinement criterion established in order to get satisfactory convergence results. In this investigation, the four-layer fluid domain division is utilized in all simulations because it combines an acceptable computation time with reasonable accuracy. The mesh distributions in the radial, circumferential, and axial directions are 4 × 360 x 40.

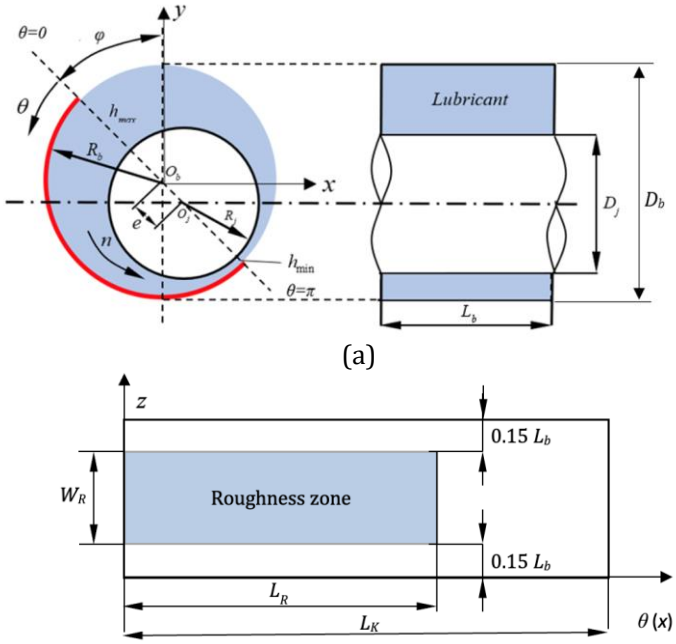

Figure 1: (a) Configuration of journal bearing with surface roughness, (b) Artificial roughness zone.

Table 1: Parameters of the model.

Parameter	**Symbol**	**Value**
Journal diameter	D_j	80 mm
Bearing diameter	D_b	79.96 mm
Bearing length	L_b	80 mm
Bearing clearance	C	0.04 mm
Eccentricity ratio	ε	0.6
Attitude angle	ϑ	30 degree
Rotational speed	n	1000 rpm
Lubricant density	ρ	998.2 kg/m^3
Lubricant viscosity	μ	0.001 Pa.s
Vapor density	ρ_v	0.552 kg/m^3
Vapor viscosity	μ_v	1.34x10^{-5} Pa.s
Saturation pressure	P_{sat}	4,042 Pa
Width of the roughness zone	W_R	56 mm
Length of the roughness zone	L_R	125.6 mm
Circumferential length of the bearing	L_K	πD_b mm
Roughness level	R_a	0 µm (perfectly smooth), 0.4 µm (fine), 1.6 µm (medium)

Table 2: Specification of the domain meshing.

Mesh criteria	**Number**
Body sizing	0.0005
Face sizing	4-layers of division
Multizone	Hexagonal
Element number	391,272
Node number	401,600
Maximum skewness	0.97739
Minimum skewness	2.388×10^{-3}

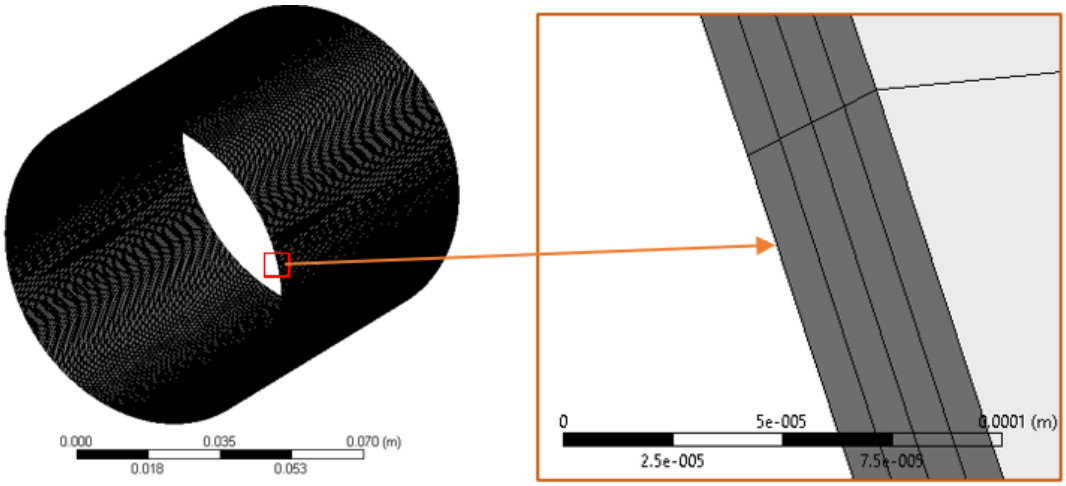

Figure 2: Grid of the domain.

Figure 3 depicts the boundary condition setup for the computational domain. In this investigation, the journal rotates at a speed n relative to the stationary bearing surface. Using pressure-inlet (marked by number 1) and pressure-outlet (denoted by number 2) boundary conditions, simulations are executed. The pressure values at the inlet and outlet are assumed to be the ambient pressure or zero (gauge) pressure. In this case, the velocity of the water inner surface (indicated by number 3) moves at the same speed as the journal, while the outer surface of the water lubricant (shown by number 4) is stationary. For moving wall boundary conditions, the rotating speed of the surface is set to 1,000 rpm. This study applies the no-slip boundary condition to the entire surface. The roughness height K_s is used as an input to represent the level of surface roughness in the roughness region (denoted by number 5).

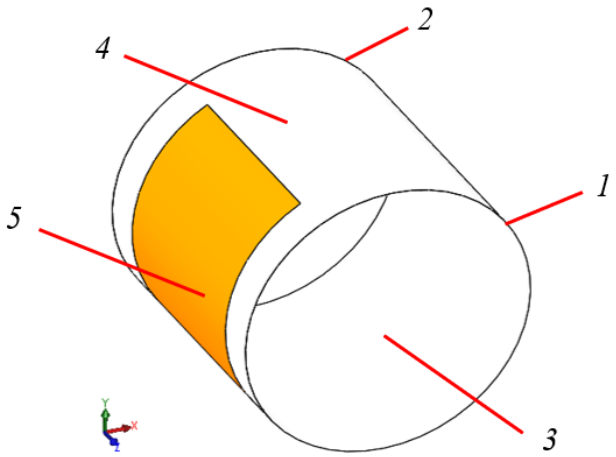

Figure 3: Boundary condition. 1—inlet, 2—outlet, 3–moving wall, 4—stationary wall, 5-roughness zone.

In the present investigation, the governing equations are discretized using the finite volume method in ANSYS FLUENT. For the velocity–pressure coupling, the SIMPLE scheme is used to obtain an accurate pressure. Furthermore, the momentum and volume fraction equations, and turbulent indices (i.e. turbulent kinetic energy and turbulent dissipation rate) are discretized with a second-order upwind scheme.

4.0 RESULTS AND DISCUSSION

The CFD numerical code including the multiphase cavitation model used in this simulation is validated to ensure correctness and accuracy. By contrasting the computed findings with those from previously published literature, the created CFD model has been validated. In this study, the dimensionless hydrodynamic pressure of the conventional smooth bearing, presented by Lin et al. (2015) is used as a reference. The comparison result, as reflected in Figure 4, shows that the values obtained from the method developed here are very similar to the reference. In terms of the maximum pressure, their deviations are less than 5% suggesting that the developed CFD code is valid.

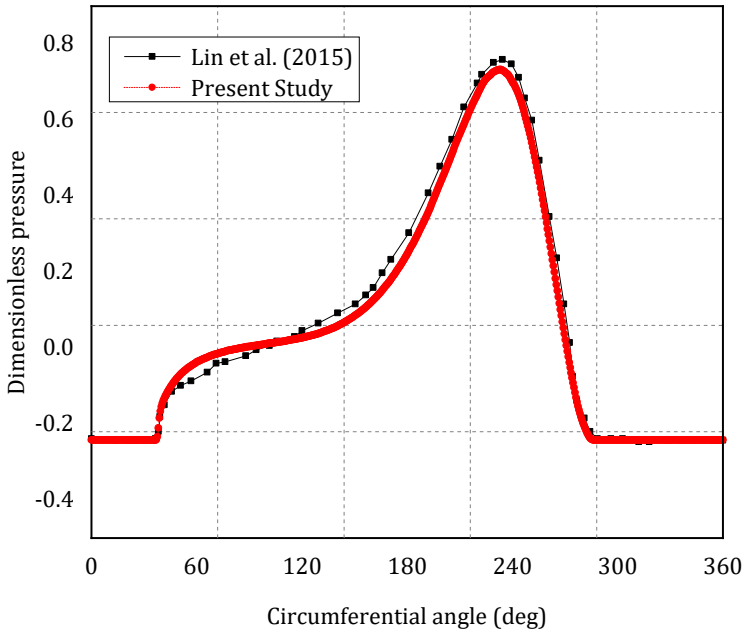

Figure 4: Comparison between the result of the present study and the literature (Lin et al., 2015).

Figure 5 depicts the load carrying capacity as a function of surface roughness level from the level of "smooth" to "medium" as indicated in Table 1 for two values of eccentricity ratios (ε=0.6 and ε = 0.4). It can be highlighted from Figure 5 that when the surface roughness level is increased, the improvement in load-carrying capacity is noted. This holds for both ε = 0.6 and ε = 0.4. The enhancement of the load-carrying capacity becomes significant when the level of surface roughness falls in the "medium" category. For example, in the case of a high eccentricity ratio (ε = 0.6 in this case). the traditional (smooth) journal bearing generates a load-carrying capacity of 512.7 N, but when the proposed design of journal bearing is employed with the R_a of 1.6 µm, the load-carrying capacity becomes 722.2 N. There is nearly a 40% improvement compared to the traditional bearing. In the case of a lower eccentricity ratio (ε = 0.4), the enhancement is more pronounced when R_a of 1.6 µm is employed. There is a 370% increase in the load-carrying capacity by using a new design of bearing in comparison to the traditional bearing.

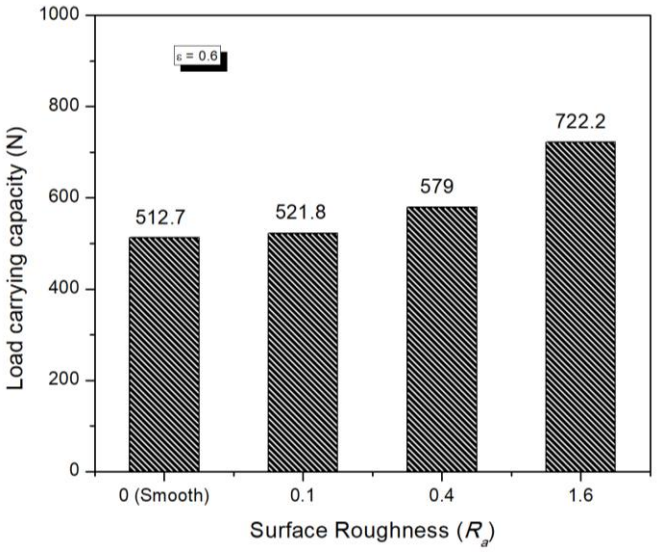

(a)

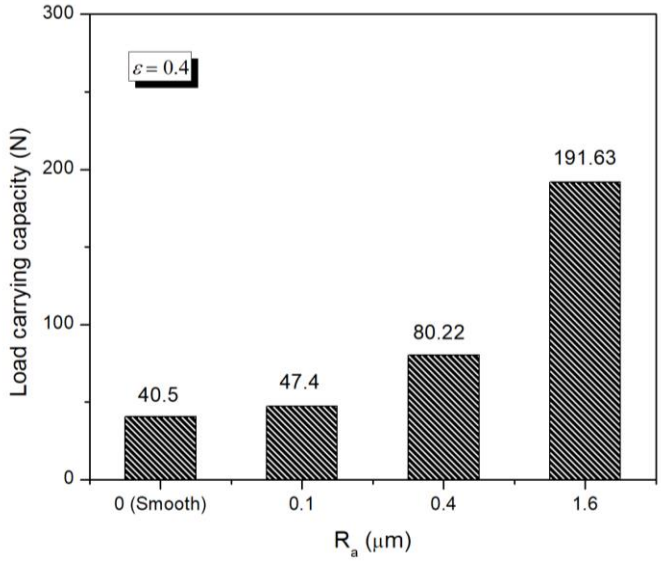

(b)

Figure 5. Load carrying capacity as a function of the surface roughness level for the case, (a) ε = 0.6 and (b) ε = 0.4.

To explore more deeply the characteristics of the load carrying capacity affected by the surface roughness, the hydrodynamic pressure profiles varying the surface roughness levels are shown in Figure 6. For two cases of eccentricity ratio considered here, it can be revealed that the maximum hydrodynamic pressure increases with increasing the surface roughness level R_a. The

increase in the maximum pressure becomes significant when the R_a of 1.6 μm is applied. When the specific surface becomes rougher, the maximum pressure increases by 7.3% and 3.4% compared to conventional journal bearings (R_a = 0 μm), respectively for ε = 0.6 and ε = 0.4. The most notable finding is that the length of the cavitation zone does not change very much with the increase in R_a. Figure 7 provides a clearer illustration of the vapor volume fraction for the case of ε = 0.6 and ε = 0.4. From the figure, it can be seen that there are two shifts in the phase change region at the beginning and end of the divergent region. This is what makes the width of the cavitation region the same for all R_a values. These two combined effects cause the load-carrying capacity to increase as the roughness value increases.

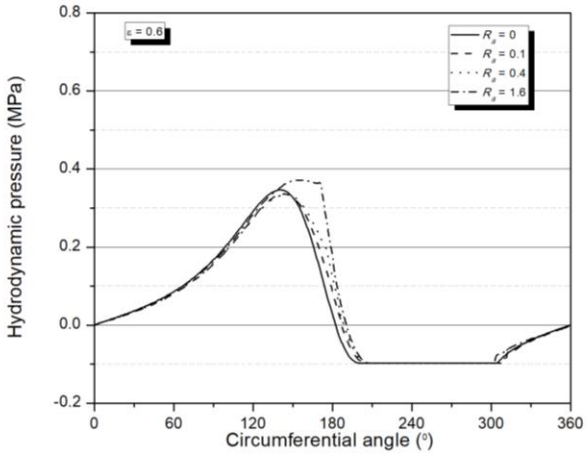

(a)

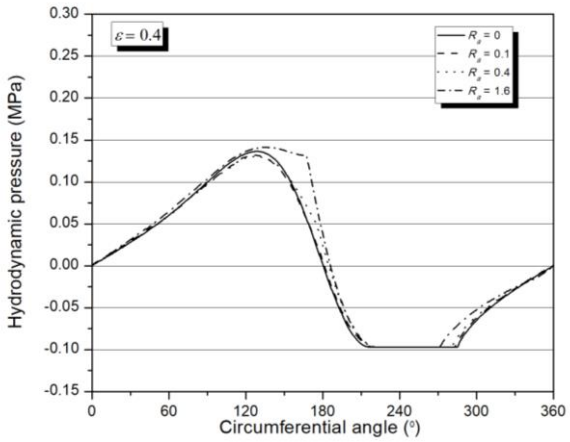

(b)

Figure 6: Hydrodynamic pressure profile of journal bearing varying the surface roughness levels for the case of (a) ε = 0.6 and (b) ε = 0.4. All results are evaluated at the mid-plane of the bearing.

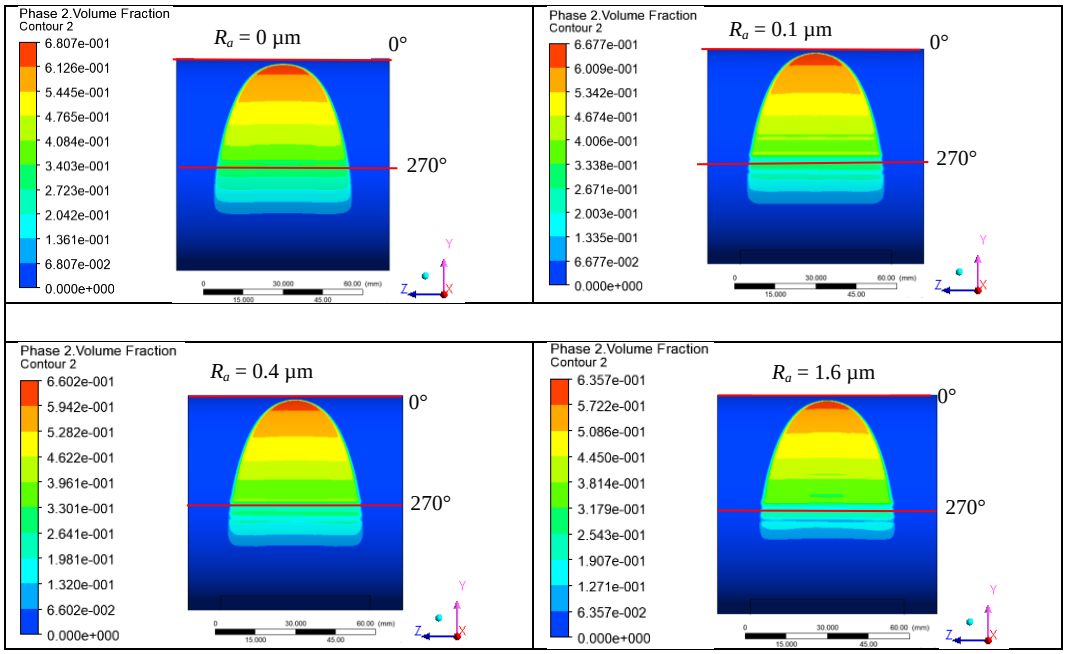

(a)

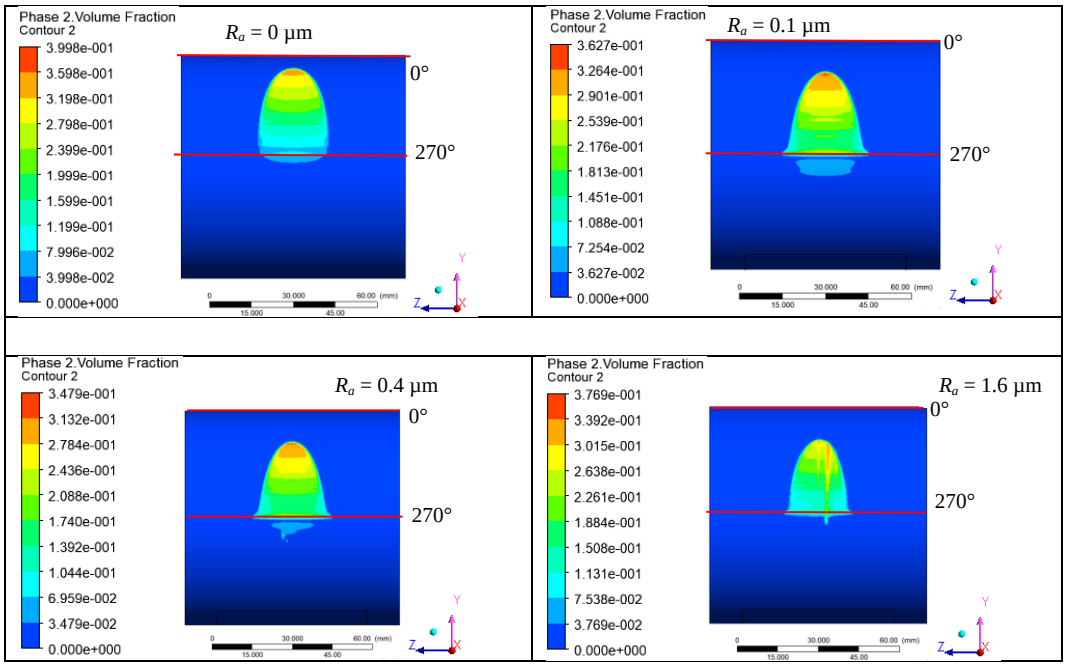

(b)

Figure 7: Vapor volume fraction of journal bearing for different roughness levels (a) in the case of ε = 0.6, and (b) ε = 0.4.

Figure 8 shows the effect of the level of surface roughness on the friction force of the new journal bearing design for two cases of eccentricity ratios. Based on Figure 8, irrespective of the eccentricity ratio considered here, it can be observed that the friction force reduces with the increase in the surface roughness level. Similar to the load-carrying capacity, the positive performance, i.e. lowest friction force is achieved when the roughness level falls into the "medium" category (R_a μm is 1.6 μm in this case). The most possible explanation is due to the deformation of the asperity. The level of surface roughness will increase the thickness of the water fluid film, which will provide a smaller contact area leading to reduced friction force. To strengthen this statement, however, it is necessary to analyze solid contact mechanics, which is our next research objective. Compared to smooth bearing, the friction reduction for ε = 0.6 and ε = 0.4 is 13% and 4%, respectively, as shown in Figure 8.

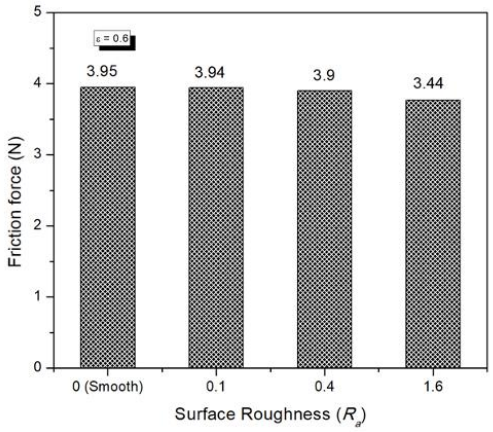

(a)

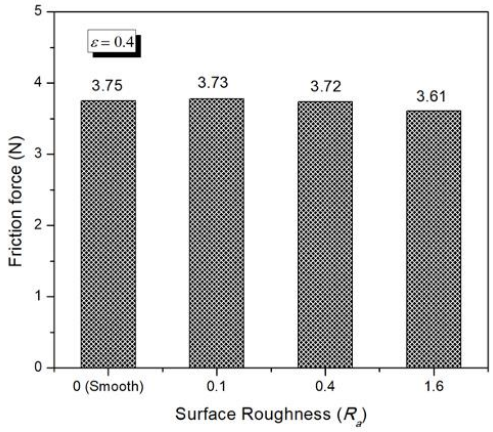

(b)

Figure 8: Friction force as a function of surface roughness level for the case of (a) ε = 0.6, and (b) ε = 0.4.

Figure 9 reflects the effect of the surface roughness level on the noise performance of the new design of journal bearing for two values of eccentricity ratios. It can be observed from Figure 9

that the average acoustic power level as a noise indicator decreases as the roughness level increases. When the surface roughness is at a "medium" level, the noise is at its lowest level. It seems that when the new design of journal bearing is employed, compared to traditional journal bearing, the noise reduces from 1 to 6% depending on the roughness level and eccentricity ratio. From the acoustic point of view, this situation has a positive effect on the environment. Again, similar to the trend of load-carrying capacity and the friction force, it can be seen that the large R_a value indicating a "rough" surface is recommended to be used when creating a journal bearing design with a partially roughened zone.

Figure 10 depicts the distribution of acoustic power levels predicted at the mid-plane of bearings (z/L_b = 0.5) with varying surface roughness levels in the case of ε = 0.6 and ε = 0.4. There are two aspects to Figure 10 that are quite eye-opening. Firstly, it reveals that, for the two eccentricity ratios considered here, due to the edge of the roughened zone, the acoustic power level increases abruptly, especially for a greater R_a. This effect makes the turbulence indicators in the divergent region more pronounced. Secondly, In the diverging region, fluctuation of surface acoustic power level for all roughness levels is also seen. This can be explained by the fact that the lubrication layer ruptures in the diverging area of journal bearings. The cavitation may cause a minor disruption to the flow pattern in that zone.

As observed in this study, employing roughness for reducing bearing noise can be a promising method for designing journal bearings. This finding is in good agreement with the recent literature. Numerically, as demonstrated by Meng et al. (2016), in the case of textured journal bearing, the dimple can decrease the acoustic power level of the bearing. Contrary to a smooth surface, the use of texture causes a sharp fluctuation in the acoustic power level. This texturing characteristic is similar to the roughness behavior in our study. Furthermore, experimentally, it has been demonstrated that a properly chosen groove can reduce noise (Meng et al., 2019; Xue et al., 2020).

To summarize the beneficial design of journal bearing with surface roughness, the performance ratio of the bearing is presented in Figure 11. Here, the performance ratio is defined as the ratio of the performance of the new design of journal bearing over the traditional journal bearing. Based on Figure 11, it can be observed that the positive behavior of the new design of journal bearing becomes significant when the level of surface roughness increases both for tribological performance (i.e. load support and friction force) and the acoustical performance (i.e. average acoustic power level). When surface roughness falls into the "fine" category, the improvement is not as substantial. But when the roughness falls to “medium” level, the performance of bearing becomes remarkable. This prevails both for low and high eccentricity ratio. Based on these results, it appears that the new design of journal bearing with a partially roughened zone is a promising means of achieving high load-carrying capacity while minimizing friction and noise.

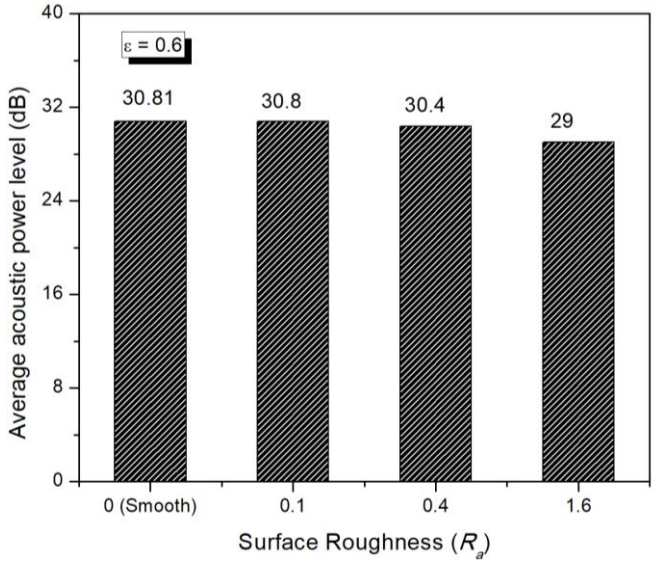

(a)

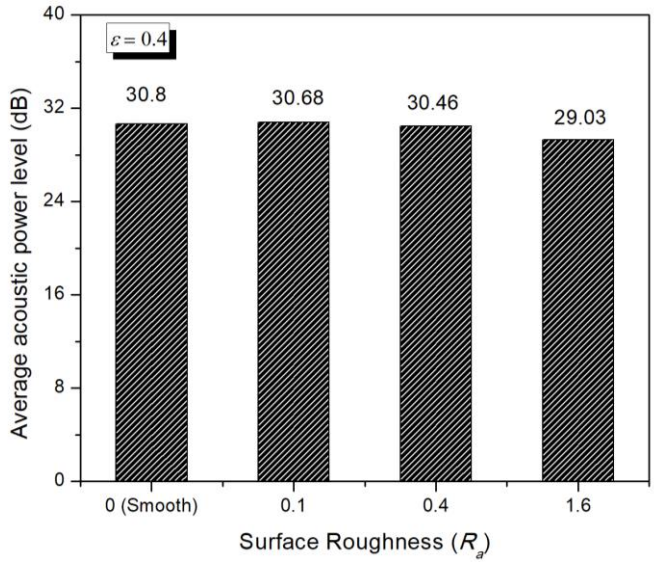

(b)

Figure 9: Acoustic power level as a function of surface roughness level in the case of (a) ε = 0.6, and (b) ε = 0.4.

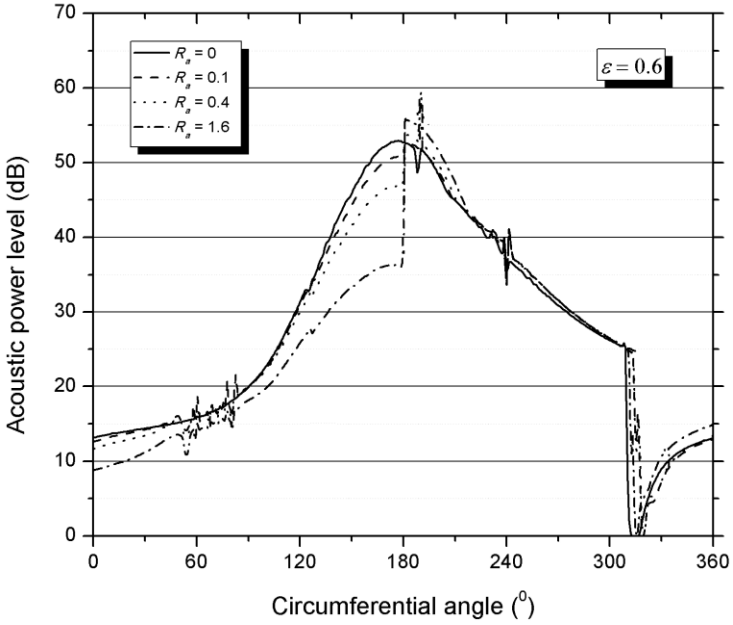

(a)

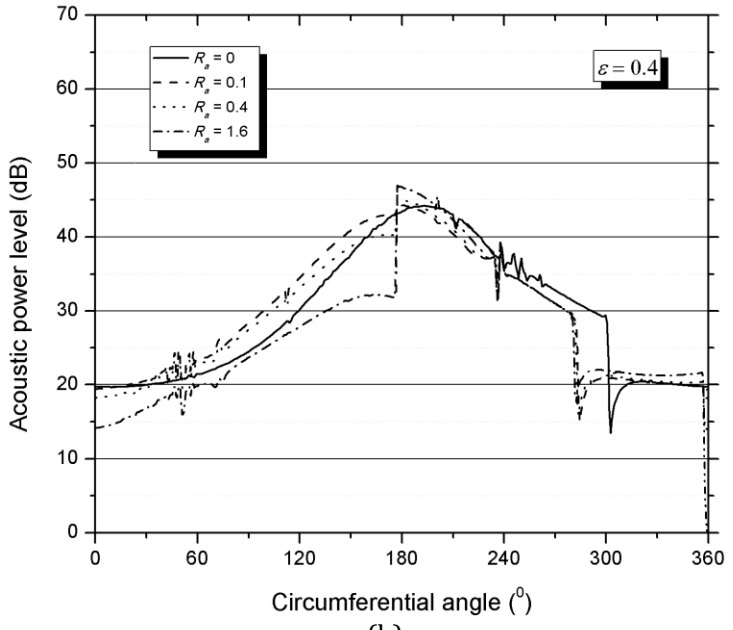

(b)

Figure 10: Acoustic power level profile of journal bearing varying surface roughness levels for the case of (a) ε = 0.6, and (b) ε = 0.4. All results are evaluated at the mid-plane of the bearing.

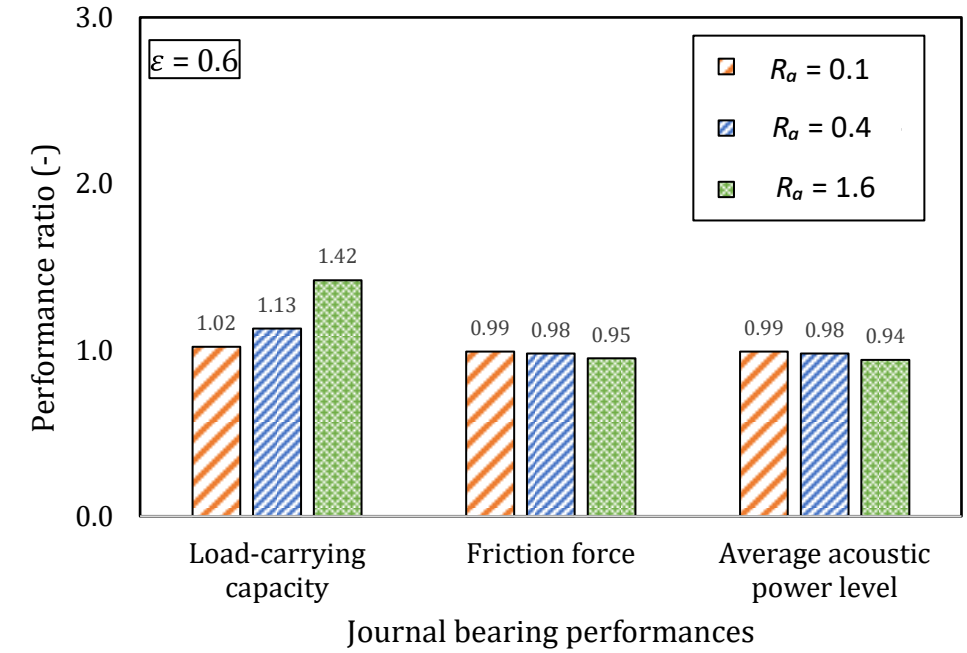

(a)

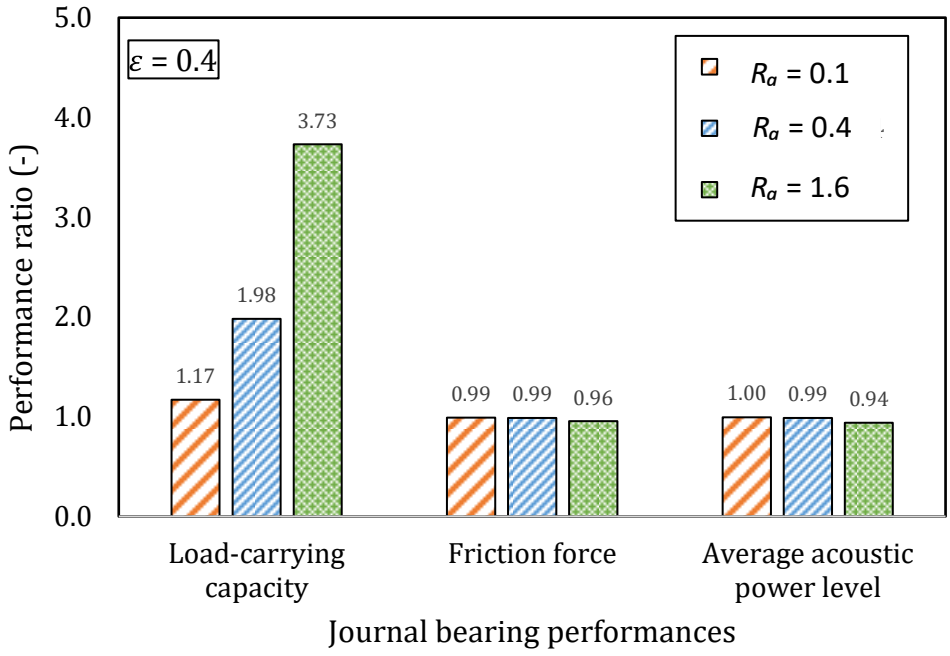

(b)

Figure 11: Performance ratio of the new design of journal bearing with surface roughness in comparison to the classical journal bearing for the case: (a) ε = 0.6, and (b) ε = 0.4

CONCLUSIONS

This study examines the performance of the new design of journal bearing with surface roughness by computational fluid dynamics (CFD). In terms of average acoustic power level, load-carrying capacity, and friction force, the behavior of the partially roughened journal bearing is evaluated by varying the surface roughness levels R_a. The numerical results indicate that a journal bearing with a partially roughened zone has an advantage over a conventional bearing both for acoustic and tribological performance regardless of the surface roughness level. The positive effect of the application of engineered roughness, that is, high carrying capacity, low friction, and low noise is more pronounced for high surface roughness levels. In comparison to the traditional journal bearing, the new design of journal bearing results in up to 1 to 4 times greater load carrying capacity, 0.95 times less frictional force, and 0.94 times less acoustic power level, depending on the eccentricity ratio, for optimal roughness level (i.e. R_a = 1.6 μm).

This study constitutes a first step toward dealing with the bearing performance of an artificially roughened bearing using a numerical approach. The experimental validation for the numerical results as discussed here will be addressed in future work.

REFERENCES

Abd Al-Samieh, M. F. (2019). Surface roughness effects for Newtonian and non-Newtonian lubricants. Tribology International, 41, 56–63.

Adams, T., Grant, C., & Watson, H. (2012). A Simple algorithm to relate measured surface roughness to equivalent sand-grain roughness. International Journal of Mechanical and Mechatronics, 1, 66-71.

ANSYS. (2019). ANSYS Fluent, version 19.0: user manual. ANSYS, Inc., Canonsburg, USA.

Cui, S., Gu, L., Fillon, M., Wang, L. & Zhang, C. (2018). The effects of surface roughness on the transient characteristics of hydrodynamic cylindrical bearings during startup. Tribology International, 128, 421–428.

Gropper, D., Wang, L., & Harvey, T. J. (2016). Hydrodynamic lubrication of textured surfaces: A review of modeling techniques and key findings. Tribology International, 94, 509-529.

Gu, C., Meng, X., Wang, S., Ding, X. (2021). Study on the mutual influence of surface roughness and texture features of rough-textured surfaces on the tribological properties. Proceedings of the Institution of Mechanical Engineers, Part J: Journal of Engineering Tribology, 235, 256–273.

Hsu, T. C., Chen, J. H., Chiang, H. L., & Chou, T. L. (2013). Lubrication performance of short journal bearings considering the effects of surface roughness and magnetic field. Tribology International, 61, 169–175.

Javorova, J. (2010). EHD lubrication of journal bearings with rough surfaces. In Proceedings of the International conference “Mechanical Engineering in XXI Century”, Nis, Serbia.

Kalavathi, G. K., Dinesh, P. A. & Gururajan, K. (2016). Influence of roughness on porous finite journal bearing with heterogeneous slip/no-slip surface. Tribology International, 102, 174–181.

Lin, Q., Wei Z., Wang N., & Chen, W., (2015), Effect of large-area texture/slip surface on journal bearing considering cavitation. Industrial Lubrication and Tribology, 67(3), 216–226

Malcolm, E. & Leader, P.E. (2001). Understanding journal bearings; Applied machinery dynamics Co.: Durango, CO, USA.

Meng, F., Wei, Z., Minggang, D., & Gao, G. (2016). Study of acoustic performance of textured journal bearing. Proceedings of the Institution of Mechanical Engineers, Part J: Journal of Engineering Tribology, 230(2), 156–169.

Meng, F., Yu, H., Gui, C., & Chen, L. (2019). Experimental study of compound texture effect on acoustic performance for lubricated textured surfaces. Tribology International, 133, 47–54.

Morris, N. J., Shahmohamadi, H., Rahmani, R., Rahnejat, H., & Garner, C.P. (2018). Combined experimental and multiphase computational fluid dynamics analysis of surface textured journal bearings in mixed regime of lubrication. Lubrication Science 30, 161–173.

Sun, D., Li, S., Fei, C., Ai, Y., Liem, R. P. (2019). Investigation of the effect of cavitation and journal whirl on static and dynamic characteristics of journal bearing. Journal of Mechanical Science and Technology, 33, 77–86.

Tauviqirrahman, M., Jamari, J., Wicaksono, A. A. Muchammad, M., Susilowati, S., Ngatilah, Y., & Pujiastuti, C. (2021). CFD Analysis of journal bearing with a heterogeneous rough/smooth surface. Lubricants, 9, 88.

Xue, Y., Shi, X., Zhou, H., Lu, G., & Zhang, J. (2020). Effects of groove-textured surface combined with Sn–Ag–Cu lubricant on friction-induced vibration and noise of GCr15 bearing steel. Tribology International, 148, 106316.